Supplementary Information (SI) for Journal of Materials Chemistry A.

Supporting Information

for

MXene-Enhanced PEGDA Crosslinked Quasi-Solid Electrolytes: A Flame-Retardant 3D Network for High-Performance Sodium-Ion Batteries

Lin Chen [a#], Yirou Du [c#], Yuhui Xie [a,b*], Guowei Jia [a], Yuanzhi Zhu [a,b], Dong Feng [a,b], Yang Meng [a,b], Yi Mei [a,b], Delong Xie [a,b*]

[a]*Faculty of Chemical Engineering, Yunnan Provincial Key Laboratory of Energy Saving in Phosphorus Chemical Engineering and New Phosphorus Materials, The International Joint Laboratory for Sustainable Polymers of Yunnan Province, Kunming University of Science and Technology, Kunming 650600, China.*

[b]*Yunnan Technological Innovation Center of Phosphorus Resources, Kunming 650600, China.*

[c]*TianfuJiangxiLaboratory，School of Physics, University of Electronic Science and Technology of China, Chengdu, 641419, China.*

# These two authors (L. Chen and Y. Du) contribute equally to this paper

*Corresponding authors:

E-mail addresses: yuhuixie@kust.edu.cn (Y. Xie), cedlxie@kust.edu.cn (D. Xie)

Electrochemical Measurements:

The ionic conductivity (σ) of the QSE was determined using AC impedance measurements on an electrochemical station (CHI 660E, CH Instruments, China) in the frequency range of 0.1 Hz to 1 MHz at 10 mV sinusoidal amplitude. Tests were carried out on the cell by sandwiching the QSE between two stainless steel (SS-316) electrodes in a 2032 coin cell. The value of σ for the QSEs was determined using Equation (1):

$$\sigma = \frac{L}{S \cdot R_b} \tag{1}$$

R_b (Ω) is the bulk ohmic resistance of the electrolyte obtained from impedance spectroscopy, and L and S are the thickness of the electrolyte (cm) and the surface area of the working electrode (cm^2), respectively. The electronic conductivity of the QSE was measured by DC polarization test by applying a voltage of 1 V in the symmetrical stainless steel 316L blocking electrode separated by the QSE under test. The electronic conductivity (Y) of the QSE was calculated by the following Equation (2):

$$Y = \frac{Is \cdot L}{E \cdot A} \tag{2}$$

I_s, L, E, and A are the steady-state current, the distance between electrodes (thickness of QSE), and the applied surface area of the working electrode, respectively.

The electrochemical stability window (ESW) of the QSEs was determined using linear scanning voltammetry (LSV) at a scan rate of 10 mV s^{-1} at 30 °C on a CHI 660E electrochemical workstation (CH instruments, China). The cells used for testing were assembled by sandwiching the QSEs between stainless steel and sodium metal in a 2032 button cell.

The Na-ion transference number t_{Na^+} was determined using chronoamperometry measurements and ac impedance of Na||QSE||Na symmetric cells conducted on the CHI 660E electrochemical workstation (CH instruments, China). t_{Na^+} can be obtained according to the following Equation (3):

$$t_{Na^+} = \frac{I_{ss}(\Delta V - I_0 R_0)}{I_0(\Delta V - I_{ss} R_{ss})} \tag{3}$$

where ΔV is the applied potential of 10 mV, I_0 and I_{ss} are the initial perturbation and steady-state currents, and R_0 and R_{ss} are the electrode/electrolyte interface resistance before and after polarization, respectively. The activation energies were calculated from the slopes of the linearly fitted curves of lnσ and 1000/T data points over the temperature range of 20 to 60 °C, the based on the Arrhenius relationship as in Equation (4):

$$\sigma = \sigma_0 \exp\left(\frac{-E_a}{kT}\right) \tag{4}$$

In Equation the term σ_0 is the pre-exponential factor of conductivity, E_a denotes the activation energy associated with Na^+ transport, k signifies the Boltzmann constant, and T represents the temperature in Kelvin.

Table S1. The components of different QSE samples.

Sample	Components
QSE-0M	PVHF, PEGDA
QSE-1M	1 wt% MXene, PVHF, PEGDA
QSE-1.5M	1.5 wt% MXene, PVHF, PEGDA
QSE-2M	2 wt% MXene, PVHF, PEGDA

Note: All samples contain EMIM-TFSI and Na-TFSI (2:1 wt), PVHF and PEGDA (1:1.5 wt).

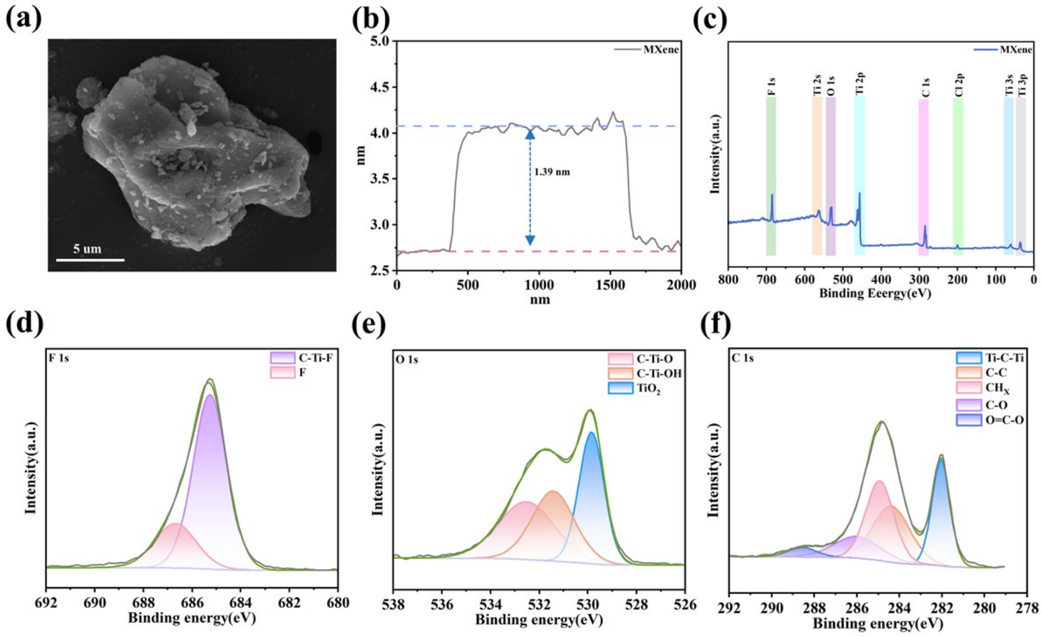

Figure S1. (a) Schematic diagram of SEM images of MAX. (b) Height of the MXene counterpart in the AFM image. (c) XPS spectra of the MXene samples. XPS data spectra showing fine maps of three elements, (d) F 1s, (e) O 1s and (f) C 1s.

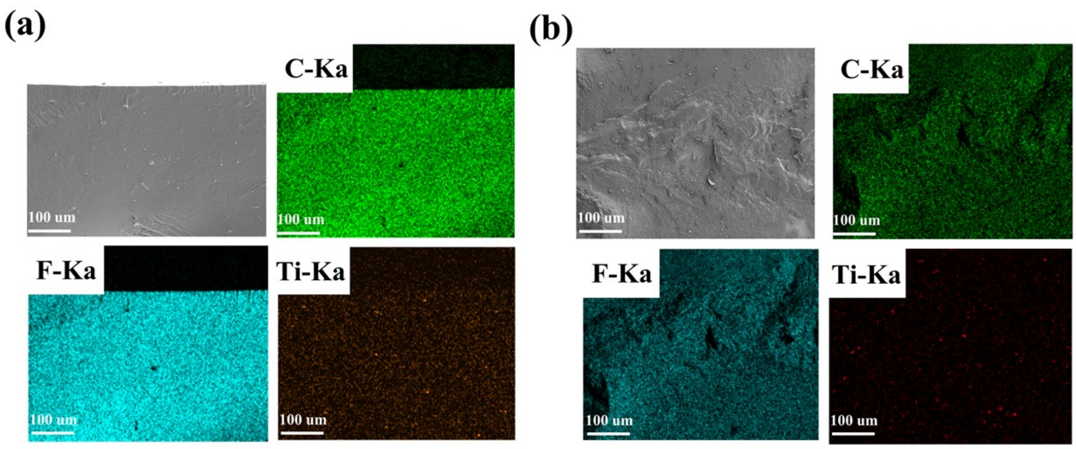

Figure S2. (a) shows the cross-sectional SEM of QSE-1.5M (1.5 wt% MXene-added QSE) and its corresponding EDS spectrum. (b) shows the cross-sectional SEM of QSE-2M (2 wt% MXene-added QSE) and its corresponding EDS spectrum.

Table S2. Results of the TGA and MCC tests.

Sample	**PHRR** (W/g)	**THR** (kJ/g)	$\boldsymbol{T}_{\mathbf{initial}}$ (°C)	**Char yield** (%)
PVHF	274.22	6.8	444.2	19.14
P(PEGDA)	392.79	23.31	334.6	3.71
MXene	/	/	632.5	93.2
QSE-0M	224.7	8.69	363.5	12.56
QSE-1M	193.28	8.45	365.2	13.92
QSE-1.5M	181.29	7.46	371.2	15.21
QSE-2M	164.57	6.8	372	16.33

$T_{initial}$: the temperature of 5% weight loss.

Table S3. LOI values of composite QSE films.

Items	QSE-0M	QSE-1M	QSE-1.5M	QSE-2M
Temperature	25 ℃	25 ℃	25 ℃	25 ℃
Ignition gas	Butane	Butane	Butane	Butane
LOI (%)	23.3	25.3	25.9	26.3
Combustion	Burn to half of the samples before self-extinguishing			

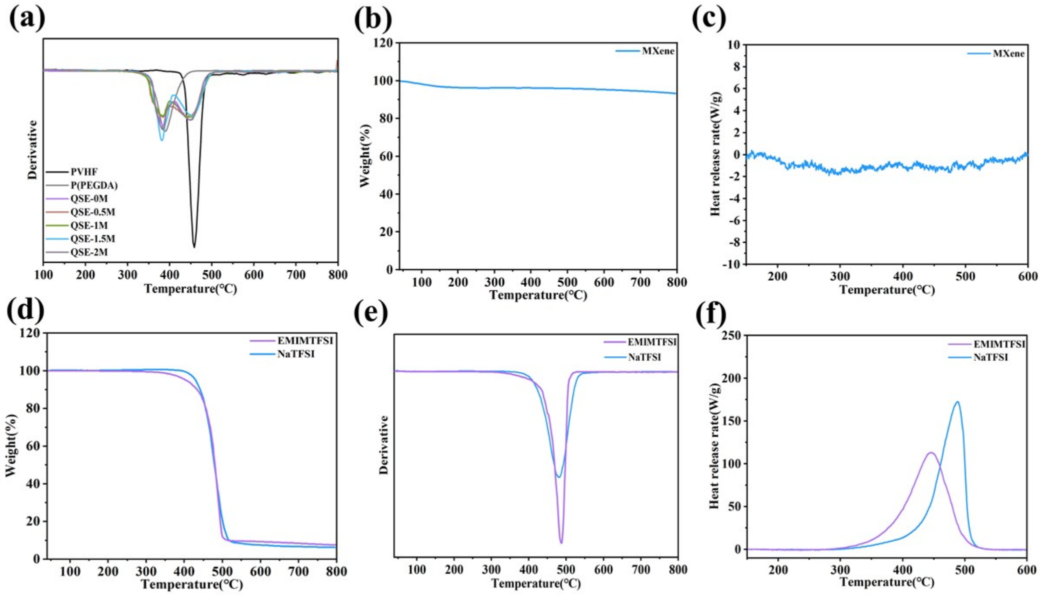

Figure S3. (a) DTG profiles of QSEs. (b) TGA profiles of MXene nanosheets. (c) Heat release rate versus temperature curves of MXene nanosheets. (d) TGA and (e) DTG profiles of EMIM-TFSI, NaTFSI. (f) Heat release rate versus temperature curves of EMIM-TFSI, NaTFSI.

Table S4. Mechanical properties of QSE samples.

Sample	**Tensile strength** (Mpa)	**Young's modulus** (Mpa)	**Elongation at break** (%)
QSE-0M	0.81	0.27	94.4
QSE-1M	0.4	0.36	127.37
QSE-1.5M	1.07	0.67	149

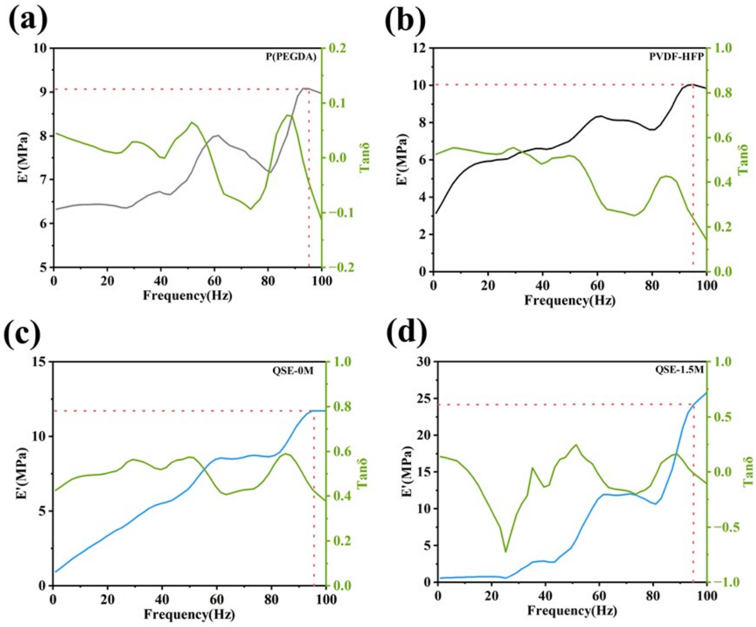

Figure S4.DMA results of (a) P(PEGDA), (b) PVDF-HFP, (c) QSE-0M and (d) QSE-1.5M.

Table S5. Result of DMA

Sample	**E'** (Mpa)	$\boldsymbol{\nu_e}$ **(× $\mathbf{10^{-4}}$ mol $\mathbf{m^{-3}}$)**
PVDF-HFP	10.05	7.3
P(PEGDA)	9.03	6.5
QSE-0M	11.71	8.7
QSE-1.5M	24.82	17.5

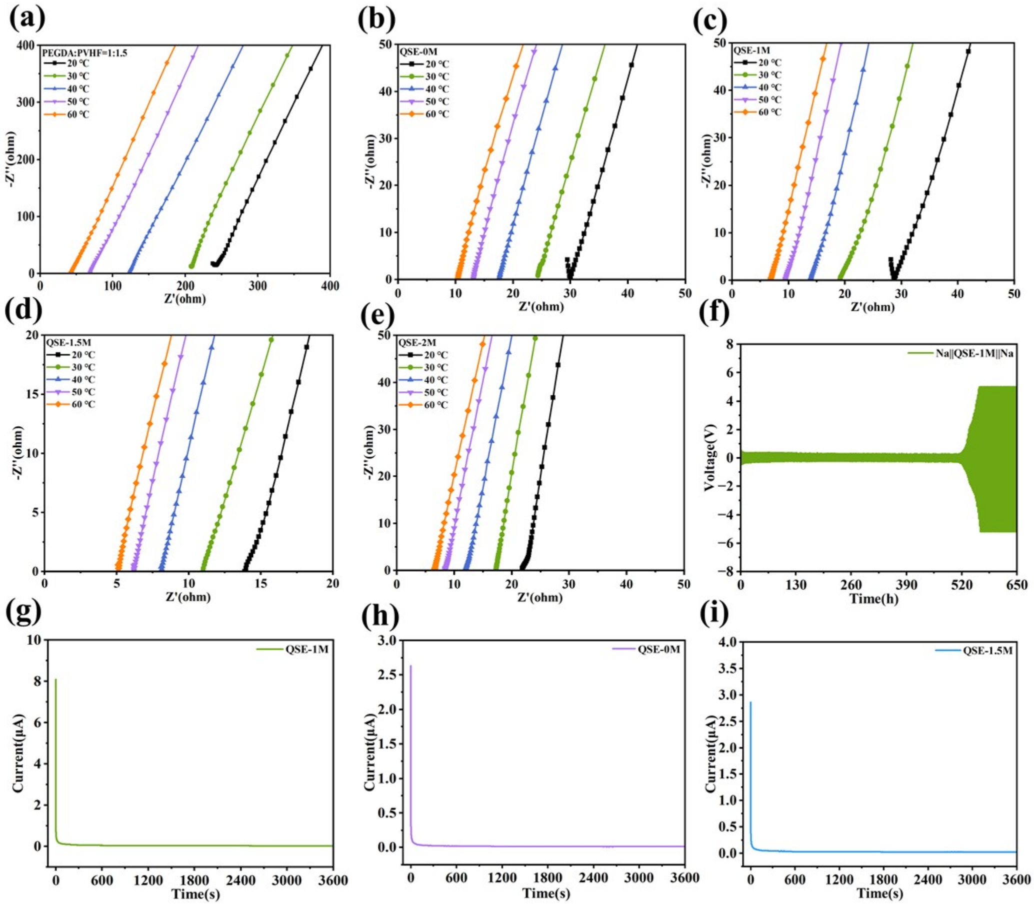

Figure S5. The Nyquist profiles of (a) P(PEGDA)-PVHF, (b) QSE-0M, (c) QSE-1M, (d) QSE-1.5M and (e) QSE-2M from 20 to 60 ℃. (f) Polarization tests of Na||QSE-1M||Na symmetric cells at current density of 0.1 mA cm^{-2}. The electronic conductivity of (g) QSE-0M, (h) QSE-1M and (i) QSE-1.5M at 30 ℃.

Table S6. Ionic conductivities at varying temperature and activation energy for the QSEs.

	Ionic conductivity *σ* (mS cm^{-1})					***E*$_a$**
Temperature (°C)	20	30	40	50	60	(eV)
P(PEGDA)-PVHF	0.041	0.048	0.081	0.144	0.233	0.456
QSE-0M	0.33	0.40	0.56	0.75	0.95	0.236
QSE-1M	0.34	0.52	0.71	1.04	1.42	0.305
QSE-1.5M	0.71	1.01	1.22	1.59	1.94	0.213
QSE-2M	0.46	0.57	0.83	1.17	1.51	0.268

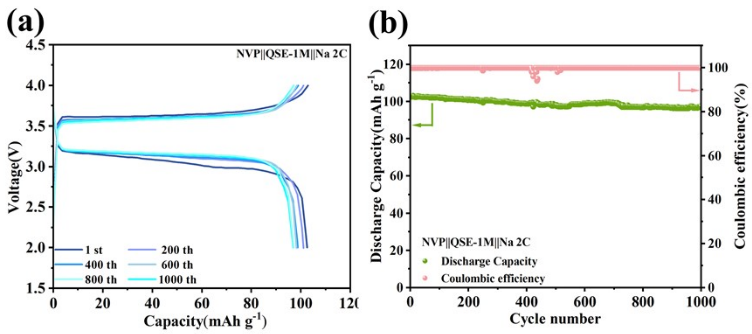

Figure S6. Capacity and efficiency versus cycle number of NVP||QSEs||Na cell at 30 °C under a current density of 2C. Charge and discharge curves of (a) QSE-1M. The corresponding cycling performances and Coulombic efficiencies are shown in (b).

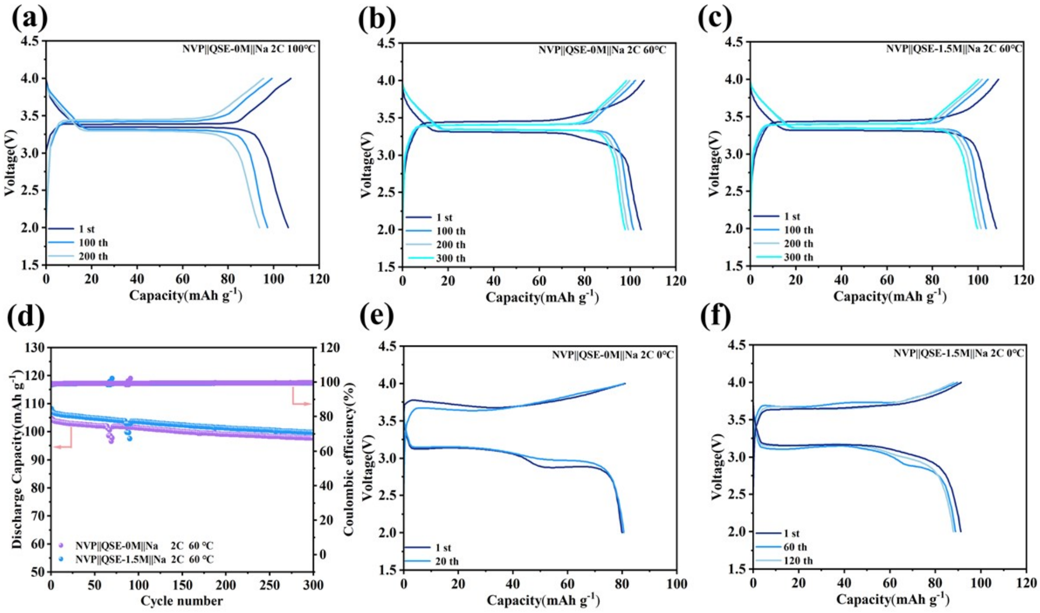

Figure S7. (a) Charge/discharge voltage curves for NVP||Na cells fitted with QSE-0M at different temperatures of 100 °C. Charge/discharge voltage curves of NVP||Na cells with QSE-0M (b) and QSE-1.5M (c) respectively at different temperatures of 60 °C. Cycling performance of QSE-0M and QSE-1.5M NVP||Na cells assembled in (d) at 60 °C. Charge/discharge voltage curves of NVP||Na cells with QSE-0M (e) and QSE-1.5M (f) respectively at different temperatures of 0 °C.

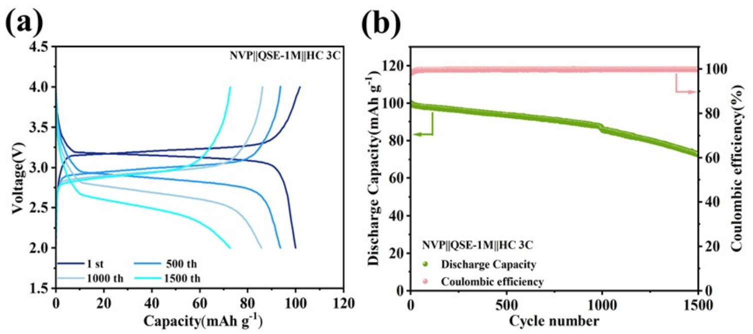

Figure S8. Capacity and efficiency versus cycle number of NVP||QSEs||HC cell at 30 °C under a current density of 3C. Charge and discharge curves of (a) QSE-1M. The corresponding cycling performances and Coulombic efficiencies are shown in (b).

Table S7. The comprehensive attributes of our work and recently reported advanced QSEs.

QSE	NVP cell performance	ESW (V)	t_{Na^+}	Elongation at break (%)	Flame retardance
This work	2500 cycles at 2 C (90.1% CR)	5.7	0.51	149	1
A-FRGPE[1]	1100 cycles at 1 C (96.1% CR)	5.63	0.68	/	1
AS-NFCGE[2]	1500 cycles at 2 C (96.6% CR)	5.37	0.28	/	1
PH-MSN-HNT[3]	100 cycles at 0.1 C (98% CR)	5.16	0.79	/	0
PEO@LM[4]	400 cycles at 0.5 C (96.3% CR)	4.60	0.17	93.62	0
PLA-NaF GPE[5]	650 cycles at 0.2 C (92.4% CR)	4.97	0.75	/	0

Note: 0 indicates inflammability, 1 indicates flame retardancy, CR indicates capacity retention.

References

1. M. Yang, F. Feng, Z. Shi, J. Guo, R. Wang, Z. Xu, Z. Liu, T. Cai, Z. Wang, C. Wang, S. Chen, Z.-F. Ma and T. Liu, *Energy Storage Mater.*, 2023, **56**, 611-620.
2. M. Yang, F. Feng, J. Guo, R. Wang, J. Yu, J. Ren, Z.-F. Ma, S. Chen and T. Liu, *Energy Storage Mater.*, 2024, **70**,103492.
3. J.-L. Gao, X.-L. Zhao, X.-Q. Ni, Y.-H. Mo, Y.-B. Tong, D.-Q. Cao, H.-B. Luo, Q. Qiao and X.-M. Ren, *ACS Appl. Energ. Mater.*, 2024, **7**, 10196-10202.
4. J. Suo, Y. Jia, X. Zhu, S. Liu, X. Tang, F. Liang, L. Wang and J. Lu, *Adv. Mater.*, 2024, **36**, 2049587.
5. X. Guo, Z. Xie, R. Wang, J. Luo, J. Chen, S. Guo, G. Tang, Y. Shi and W. Chen, *Angew. Chem.-Int. Edit.*, 2024, **63**, e202402245.